Jia-Xin Chen, Xiao-Ge Zhao, Xing-Xing Dong, Zhen-Long Lv* and Hong-Ling Cui

Density Functional Study of the Electronic, Elastic and Optical Properties of Bi₂O₂Te

https://doi.org/10.1515/zna-2019-0185 Received May 29, 2019; accepted August 26, 2019; previously published online September 17, 2019

Abstract: Layered crystal Bi₂O₂Te has recently been found to have high electron mobility and excellent thermoelectric properties for technical applications; however, its other properties are not well studied vet. In this work, the electronic, elastic and optical properties of Bi₂O₂Te are systematically studied using the density functional method. The results indicate that Bi₂O₂Te is a narrow band gap semiconductor. The gap is formed by the Te 5p orbital at the top of the valence band and the Bi 6p orbital at the bottom of the conduction band. There are both ionic and covalent interactions within the Bi-O layers, and these layers are linked by the ionic Bi-Te bonds forming the crystal. Bi₂O₂Te is mechanically stable but anisotropic. It is easy to fracture along the c axis under shear stress. Its shear modulus is far smaller than its bulk modulus, so shape deformation is easier to occur than pure volume change. Its melting point is predicted to be 1284.0 K based on an empirical formula. The calculated refractive index at zero frequency reveals that Bi₂O₂Te is a negative uniaxial crystal with a birefringence of 0.51, making it a potential tuning material for optical application. The characteristics and origins of other optical properties are also discussed.

Keywords: Density Functional Theory; Elastic Property; Electronic Property; Optical Property.

PACS: 71.15.Mb; 71.20.-b; 74.25.Ld, 78.20.Ci.

1 Introduction

Bismuth is a heavy element located at the sixth period in the periodic table, which is known for having a

*Corresponding author: Zhen-Long Lv, School of Physics and Engineering, Henan University of Science and Technology, Luoyang 471023, China, E-mail: zhenlonglv@foxmail.com Jia-Xin Chen, Xiao-Ge Zhao, Xing-Xing Dong and Hong-Ling Cui: School of Physics and Engineering, Henan University of Science and Technology, Luoyang 471023, China, E-mail: 384263318@qq.com (J.-X. Chen); 2285415584@qq.com (X.-G. Zhao); 2388238839@qq.com (X.-X. Dong); hlcui168@163.com (H.-L. Cui)

strong spin-orbit coupling effect [1, 2]. Bismuth-containing compounds usually have many peculiar properties. For example, layered Bi_2Se_3 and Bi_2Te_3 are thermoelectric materials with high thermoelectric figure of merit at room temperature [3, 4]. They are also three-dimensional topological insulators and are expected to be used in spintronic devices in the future [5, 6].

Bi₂O₂Se and Bi₂O₂Te are layered tetragonal crystals, which can be regarded as the phases transformed from their respective counterparts, Bi₂Se₃ and Bi₂Te₃, after partially substituting the element O for the element Se or Te. In 1973, Boller [7] reported synthesising Bi₂O₂Se from Bi₂O₃ and Se through a solid-state reaction for the first time, and measured its space group and lattice parameters. However, almost no research has been done on the properties of these crystals in the following decades. In 2010, Ruleova et al. [8] synthesised Bi₂O₂Se from Bi₂Se₃ and Bi₂O₃ using the solid-state reaction method. They studied the relationship between temperature and the Seebeck coefficient, conductivity and thermal conductivity of Bi₂O₂Se. They found that Bi₂O₂Se is an n-type semiconductor with a low thermal conductivity and its thermoelectric figure of merit is close to 0.2 at 800 K. Afterwards, different research groups studied the electronic property, thermal conductivity and thermoelectric property of different forms of Bi₂O₂Se, and found that many of them are promising thermoelectric materials [9-12]. In other aspects, Pereira et al. [13] studied the structural, vibrational and elastic properties of Bi₂O₂Se under high pressure by combining first-principles calculation with experiments. It is revealed that the structure of Bi₂O₂Se is stable when the external pressure increases to 30 GPa; however, the electronic properties are obviously changed at 4 GPa.

Because the crystal structures of Bi_2O_2Te and Bi_2O_2Se are the same, in addition to Te and Se belonging to the same group, one can expect that they have similar properties. In 2015, Luu and Vaqueiro [14] synthesised Bi_2O_2Te using Bi, Bi_2O_3 and Te using a solid-state reaction. The structure of the crystal was determined, and its electronic and thermal properties were measured in the temperature range of 300-665 K. It is found that the crystal is an n-type semiconductor with a band gap of 0.23 eV. Its thermal conductivity at room temperature is 0.91 W/m/K, and it has thermoelectric properties superior to those of

Bi₂O₂Se. The first-principles calculations performed by Wu and Zeng [15] show that Bi₂O₂Se and Bi₂O₂Te not only have high electron mobility but also have ferroelectric and ferroelastic properties, which can be used to fabricate nonvolatile storage devices in nanocircuits. Wang et al. [16] studied the electronic and phonon transport properties of Bi₂O₂Se and Bi₂O₂Te by using the first-principles method and Boltzmann transport theory. Their results imply that p-type doping can induce a much higher Seebeck coefficient and power factor than n-type doping. Bi₂O₂Te has a lower thermal conductivity and a higher thermoelectric performance than Bi₂O₂Se.

It can be seen that previous studies mostly focus on Bi₂O₂Se; however, the basic properties of Bi₂O₂Te, such as its bonding, elastic and optical properties, are not studied yet, although these properties are important for its potential applications. For example, we found in our study that Bi₂O₂Te is a negative uniaxial crystal with large birefringence comparable to some liquid crystals, which makes it very promising for use as a tuning material in optical fields.

2 Computational Details

2.1 Computational Settings

The Vienna Ab initio Simulation Package (VASP) code [17] is used to optimise the structure and calculate the properties of Bi₂O₂Te. Projector-augmented-wave pseudopotentials [18] are employed to describe the interaction between ions and electrons, where the electronic configuration of Bi is 5d¹⁰6s²6p³, that of O is 2s²2p⁴ and that of Te is $5s^25p^4$. The Perdew-Burke-Ernzerhof functional [19] within the generalised gradient approximation (GGA) is adopted to calculate the exchange-correlation energy of the electrons. The atomic wave functions are expanded by a group of plane waves with a truncated energy of 520 eV. Brillouin zone integral is performed on a discrete $7 \times 7 \times 7$ mesh [20] in lattice relaxation, which increases to 15 \times 15 \times 15 when calculating the electronic and optical properties. The convergence criterion of energy is set to 1×10^{-6} eV/atom, and the maximum force between ions is set to 0.01 eV/Å. The tests verify that these above parameters can ensure the convergences of the studied properties. Considering that pure density function calculations often underestimate the band gaps of materials, we use the modified Becke-Johnson (mBJ) potential [21] when studying the electronic and optical properties to make the results reasonable.

2.2 Calculation of Elastic Properties

The elastic constants of Bi₂O₂Te are calculated by the density functional perturbation method implemented in VASP. Tetragonal crystals have six independent elastic constants: C_{11} , C_{33} , C_{44} , C_{66} , C_{12} and C_{13} . For polycrystals, comprehensive physical quantities, such as bulk modulus (B) and shear modulus (G), are usually used to describe their elastic properties [22]. The methods proposed by Voigt and Reuss are commonly used in the literature to derive the bulk modulus and shear modulus of a polycrystal. Voigt's formulas for calculating the bulk modulus and shear modulus of a tetragonal crystal are as follows [22]:

$$B_V = [2(C_{11} + C_{12}) + 4C_{13} + C_{33})]/9,$$
 (1)

$$G_V = (M + 3C_{11} - 3C_{12} + 12C_{44} + 6C_{66})/30.$$
 (2)

Reuss' formulas for calculating these two moduli are as follows:

$$B_R = C^2/M, \tag{3}$$

$$G_R = 15/[18B_V/C^2 + 6/(C_{11} - C_{12}) + 6/C_{44} + 3/C_{66}],$$
 (4)

where $M = C_{11} + C_{12} + 2C_{33} - 4C_{13}$, $C^2 = (C_{11} + C_{12})C_{33} 2C_{13}^2$. In practice, the average values of the above variables are taken as the final values, i.e.

$$B = (B_V + B_R)/2$$
, $G = (G_V + G_R)/2$. (5)

Poisson's ratio of a polycrystal can be obtained using the following formula:

$$v = (3B - 2G)/(6B + 2G). \tag{6}$$

The shear wave velocity (V_t) , longitudinal wave velocity (V_l) and average wave velocity (V_m) propagating in a polycrystal can be deduced from the following formulas, respectively [23]:

$$V_l = \sqrt{(3B + 4G)/3\rho}, \ V_t = \sqrt{G/\rho},$$

$$V_m = \left[\frac{1}{3}\left(\frac{2}{V_t^3} + \frac{1}{V_l^3}\right)\right]^{-1/3}.$$
 (7)

The Debye temperature Θ , related to the thermal properties of materials, can be obtained via the following expression:

$$\Theta = \frac{h}{k_B} \left[\frac{3n}{4\pi} \left(\frac{N_A \rho}{M} \right) \right]^{1/3} V_m, \tag{8}$$

where h is the Planck constant, k is the Boltzmann constant, n is the number of atoms contained in one molecular formula, N_A is the Avogadro number, ρ is the density of the material and *M* is its molecular weight.

3 Results and Discussion

3.1 Crystal Structure

Bi $_2$ O $_2$ Te is a tetragonal crystal and its space group is I4/mmm (no. 139), as shown in Figure 1. The reported lattice constants are a=3.980 Å, c=12.704 Å, and the fractional coordinates of atoms are Bi (0, 0, 0.3472), O (0.5, 0, 0.25) and Te (0, 0, 0) [14]. One unit cell contains four Bi atoms, four O atoms and two Te atoms. The lattice constants after structural relaxation are a=4.019 Å, b=12.885 Å. The fractional coordinates of Bi are (0, 0, 0.3467) and those of other two atoms are kept unchanged due to their special high site symmetries. These three relaxed parameters are close to the experimental values with relative errors of 1.0 %, 1.4 % and -0.14 %, respectively, which could be acceptable in common density functional calculations.

3.2 Electronic Properties

The calculated band structure along the high symmetry directions in the Brillouin zone of Bi_2O_2Te is shown in Figure 2a. Because the bands near the Fermi level have the greatest influence on the electronic properties of crystals, we mainly presented the bands between -8.0 and 6.0 eV. The results show that the top of the valence band is at the

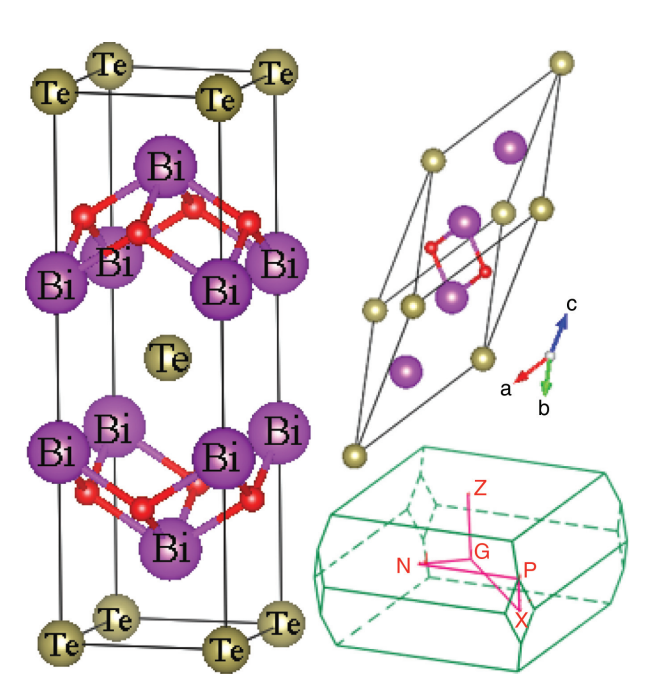
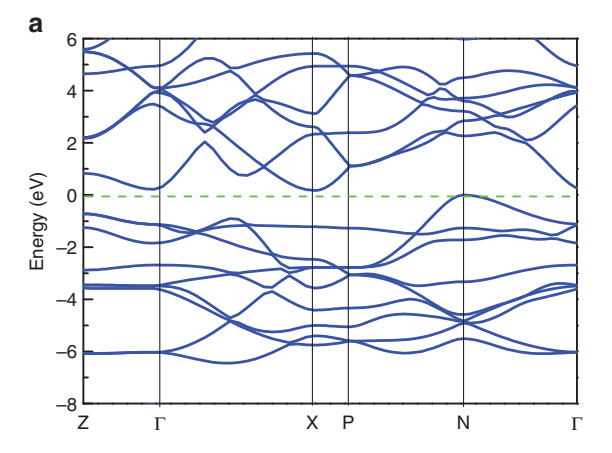


Figure 1: Crystal structure (left) and primitive cell and Brillouin zone (right) of Bi_2O_2Te . The large, medium and small balls represent the Bi, Te and O atoms, respectively.



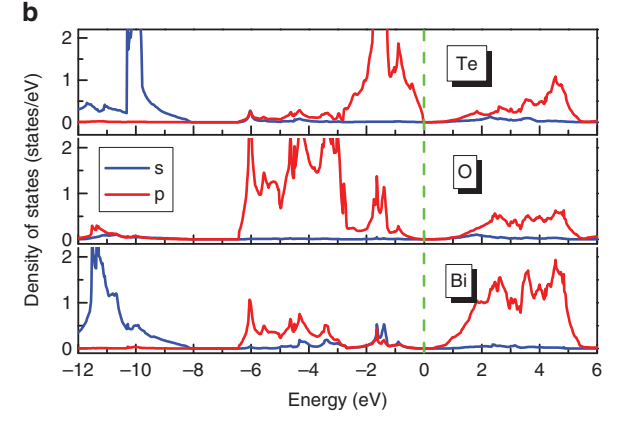


Figure 2: Calculated (a) band structure and (b) partial DOS of Bi₂O₂Te. The green dashed lines represent the Fermi level.

N point while the bottom of the conduction band is at the X point, so $\rm Bi_2O_2Te$ is an indirect crystal. The band gap calculated by the GGA functional is almost equal to zero, far smaller than the experimental value of 0.23 eV [14]. It increases to 0.20 eV when the mBJ potential is used with the GGA functional.

The band structure of Bi_2O_2Te seems dispersive. To find their origins, we calculated its density of states (DOS), as illustrated in Figure 2b. It reveals that the bands located in the energy range from -6.5 to -2.5 eV come mainly from the O 2p and the Bi 6p orbitals; the bands located between -2.5 eV and the Fermi level mainly originate from the Te 5p orbital, with a little contribution from O 2p orbital and Bi 6s and 6p orbitals; and the bands from 0.5 to 6.0 eV are mainly from the Bi 6p orbital, together with some contribution from the O 2p and the Te 5p orbitals. It can also be seen that the band gap of Bi_2O_2Te is formed by the Te 5p orbital located at the top of the valence band and the Bi 6p orbital located at the bottom of the conduction band.

From the calculated partial DOS, one can find that the overlap between the s and p orbitals within each type of

atom is rather limited, which indicates that the hybridisation in the atom itself is very weak. However, the p orbitals of the O and Bi atoms overlap seriously and have high densities in the energy range from -6.5 to -2.5 eV, which implies that there exists certain hybridisation between the p orbitals of O and Bi. The p orbital of Te is relatively localised, having high peak values in the energy range from -2.5 eV to the Fermi level. It has a weak hybridisation with the Bi 5s and 5p orbitals, indicating a very weak covalent interaction between the Te atoms and the Bi atoms. The hybridisation between the p orbitals of the constituent atoms makes the bands of Bi₂O₂Te fluctuated.

Bi₂O₂Te seems like a layered crystal, so it is meaningful to study its bonding properties. For this end, we calculated its charge density difference and displayed it in Figure 3. It is shown that the O atoms obtain electrons (blue colour) while the Bi atoms lose electrons (red colour) when forming the crystal, so there also exists an ionic interaction between the Bi and O atoms. There are no electrons accumulating between the Te and Bi atoms, suggesting that the interaction between them is ionic. The distance between the Te and Bi atoms is 3.461 Å and that between the Te and O atoms is 3.797 Å, which is much longer than the value of 2.364 Å between the Bi and O atoms, so the interaction between the Te and Bi (O) atoms is weaker than that between the Bi and O atoms. Bader analysis [24] indicates that each O atom obtains 1.16 electrons, each Te atom obtains 0.82 electrons, while each Bi atom loses 1.57 electrons. From the above analyses, we can infer that the Bi and O atoms form the Bi-O layers by ioncovalent interaction, and then these layers form the crystal mainly through the ionic interaction between the Bi and Te atoms.

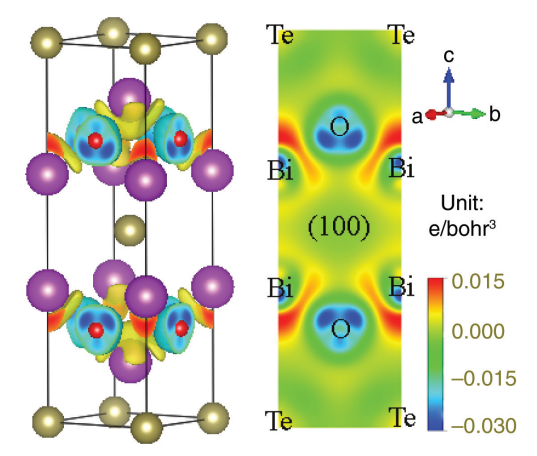


Figure 3: Charge density difference (left) and that in the (100) plane (right) of Bi₂O₂Te. The blue (negative) and red (positive) colours represent electron enhancement and depletion, respectively.

3.3 Elastic Properties

The elastic constants of materials can be used to describe their responses to external stresses within their elastic limits, which are closely related to the mechanical stability of materials. The calculated elastic constants of Bi₂O₂Te are $C_{11} = 140.3$ GPa, $C_{33} = 98.9$ GPa, $C_{44} = 24.3$ GPa, $C_{66} = 51.8 \text{ GPa}, C_{12} = 63.1 \text{ GPa} \text{ and } C_{13} = 41.5 \text{ GPa}.$ For tetragonal crystals, the criteria of mechanical stability are [22] $C_{11} > 0$, $C_{33} > 0$, $C_{44} > 0$, $C_{66} > 0$, $C_{11} - C_{12} > 0$, $C_{11} + C_{33} - 2C_{13} > 0$, $2(C_{11} + C_{12}) + C_{33} + 4C_{13} > 0$. The calculated elastic constants satisfy the above criteria, so Bi₂O₂Te is mechanically stable.

The elastic constant C_{11} is larger than C_{33} , which indicates that the stiffness of Bi_2O_2Te along the a/b axis is greater than that along the c axis. In other words, the strain of the a axis is smaller than that of the c axis when a given normal stress is applied along the a axis and thec axis, respectively. C_{12} is larger than C_{13} , which implies that the strain of the c axis is larger than that of the b axis when a given normal stress is applied along the a axis. C_{44} and C_{66} are elastic constants related to shear strain. C_{66} is larger than C_{44} , which means that the latter will produce a greater strain when the same shear stress is applied to the $[0 \pm 10](\pm 100)$ and the $[0 \pm 10](00 \pm 1)$ shear systems, respectively. The elastic constants C_{13} and C_{44} are both related to the bonding properties along the *c* axis of the crystal. C_{13} and C_{44} are the two smallest elastic constants among all, which means that the bonds along the c axis are the weakest and the crystal is easier to fracture along the *c* axis under shear stress.

Bulk modulus describes the relative volume change of a material under hydrostatic pressure, while shear modulus reflects the resistance of a material to shear deformation. The calculated bulk modulus of Bi₂O₂Te is 72.8 GPa and the shear modulus is 34.0 GPa. The former is much larger than the latter, which implies that the shear deformation is the main factor determining the mechanical stability of the crystal. Pugh [25] proposed that the brittleness and ductility of a material can be discriminated by the value of B/G. A value >1.75 means that the material is ductile, or else it is brittle. The calculated *B/G* ratio of Bi₂O₂Te is 2.14, which suggests that it is ductile. Haines et al. [26] pointed out that Poisson's ratio can be used to determine the bonding properties of materials: for pure covalent crystals, the value is around 0.1 and for ion-covalent crystals, the value is between 0.2 and 0.3. The calculated Poisson's ratio of Bi₂O₂Te is 0.3, which suggests that it is an ioncovalent crystal. This result is consistent with the conclusion drawn previously. Chen et al. [27] put forward that the hardness of a material could be estimated from its

bulk modulus and shear modulus. They gave a formula for calculating Vickers hardness: $H_{\rm v}=2(G^3/B^2)^{0.585}-3$, from which we deduced that the hardness of Bi₂O₂Te is about 3.5 GPa. The Debye temperature is closely related to the thermal properties of materials. The values of the shear, longitudinal and average wave velocities of Bi₂O₂Te calculated from the elastic constants are 1921.3, 3579.9 and 2145.4 m/s, respectively. The Debye temperature is finally predicted to be about 232.2 K. Using the empirical formula $T_{\rm m}=607+9.3\times B$ (bulk modulus) [28], we obtained a value of 1284.0 K for the melting point of Bi₂O₂Te.

Previous studies have revealed that a material is prone to cracking if its elastic anisotropy is large [29]. Therefore, it is important to study the elastic anisotropy of materials. Here, we studied the elastic anisotropy of ${\rm Bi}_2{\rm O}_2{\rm Te}$ using the directional bulk modulus and Young's modulus. The former characterises the linear compressibility of a material in all directions under a hydrostatic pressure, while the latter characterises the compressibility of a material along the direction of an applied uniaxial stress. The formulas for calculating these two quantities of tetragonal crystals are as follows [30]:

$$B = [(S_{11} + S_{12} + S_{13}) - (S_{11} + S_{12} - S_{13} - S_{33})l_3^2]^{-1},$$

$$(9)$$

$$E = [(l_1^4 + l_2^4)S_{11} + l_3^4S_{33} + l_1^2l_2^2(2S_{12} + S_{66}) + l_3^2(1 - l_3^2)(2S_{13} + S_{44})]^{-1},$$

$$(10)$$

where $(l_1 \ l_2 \ l_3)$ denotes the directional cosine and S_{ij} is the element in the elastic yield tensor matrix, which is the inverse of the elastic tensor matrix.

Figure 4 shows the directional bulk modulus and Young's modulus. Both graphs are not spherical, indicating that the elastic properties of ${\rm Bi_2O_2Te}$ are anisotropic. The maximum bulk modulus is 290.4 GPa in the (001) plane and the minimum is 138.4 GPa in the [001] direction, which means that the c axis of ${\rm Bi_2O_2Te}$ is easiest to contract under a hydrostatic pressure. The maximum

Young's modulus is 128.3 GPa in the diagonal directions of the (001) plane and the minimum is 68.6 GPa in the diagonal directions of the (100) and (010) planes, so the former directions are difficult to be compressed and stretched.

3.4 Optical Properties

The optical properties of a crystal, such as its refraction, absorption and reflection functions, can be deduced from its dielectric function $\varepsilon(\omega)$. The imaginary part of the dielectric function $\varepsilon_2(\omega)$ of a crystal can be obtained by calculating the allowable transition of electrons in Brillouin zone from the occupied orbitals to the unoccupied orbitals under an incident light [31]:

$$\varepsilon_2^{\alpha\beta}(\omega) = \frac{4\pi^2 e^2}{\Omega} \lim_{q \to 0} \frac{1}{q^2} \sum_{c,v,k} 2\omega_k \delta(E_{ck} - E_{vk} - \omega)
\times \left\langle u_{ck+c_\alpha+q} | u_{vk} \right\rangle \left\langle u_{ck+c_\beta+q} | u_{vk} \right\rangle^*,$$
(11)

where q is the Bloch vector of the light; ω is the frequency of the light; ck and vk denote the empty and occupied orbitals at the k point of the Brillouin zone, respectively; u_{ck} and u_{vk} are the cell periodic part of the orbitals at the k point; and E_{ck} and E_{vk} are the corresponding energies. The real part of the dielectric function $\varepsilon_1(\omega)$ can be obtained using the Kramers–Kronig relation:

$$\varepsilon_1^{\alpha\beta}(\omega) = 1 + \frac{2}{\pi} P \int_0^\infty \frac{\omega' \varepsilon_2^{\alpha\beta}(\omega')}{\omega'^2 - \omega^2 + i\eta} d\omega',$$
(12)

where *P* means the principal integral and η is the smearing factor with a value of 0.1.

 ${\rm Bi_2O_2Te}$ is a tetragonal crystal, so it is a uniaxial crystal with the c axis as its optical axis. When a beam of light having a polarisation direction perpendicular to the c axis propagates in it, it will have the same optical response regardless of the propagating direction. However, its optical response will be different if the transiting light has a

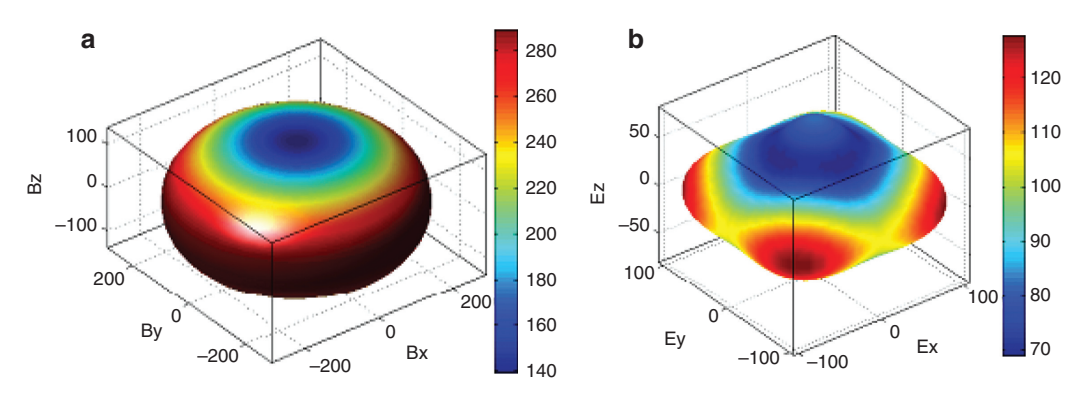


Figure 4: Directional (a) bulk modulus and (b) Young's modulus of Bi₂O₂Te (unit: GPa).

polarisation direction parallel to the c axis. In the following sections, we will use the signs " \bot " and "//" to represent the polarisation directions of lights perpendicular and parallel to the c axis, respectively. Obviously, the former relates to the case of the ordinary light while the latter connects with the case of the extraordinary light.

The calculated dielectric curves of Bi₂O₂Te are illustrated in Figure 5. For the convenience of discussion, the total DOS of Bi₂O₂Te is also given in the figure. The dielectric curves are different in the two polarisation directions. There is one apparent peak and a broad shoulder in the curves of $\varepsilon_2(\omega)$ in both cases. The peak is located at about 2.6 eV and the shoulder extends to 4.8 eV for the perpendicular polarisation case. The shoulder starts at about 2.7 eV and ends at the peak located at about 4.2 eV for the parallel polarisation case. From the calculated DOS and bond lengths, one can know that these peaks and shoulders should mainly be induced by the transition of electrons from the p orbitals of Te and O to the 6p orbitals of Bi. The curves of the parallel polarisation case shift right and meanwhile lower their values, which should be caused by the difference of the transition details of electrons under the perturbation of light. The calculated curves of $\varepsilon_1(\omega)$ reveal that the zero-frequency dielectric constants along the two directions are $\varepsilon_{\perp}=12.985$ and $\varepsilon_{//} = 9.547.$

The refraction function $n(\omega)$ determines the propagation speed of light in materials and the extinction function $k(\omega)$ reflects the attenuation of light in materials. They can be derived from the following formulas, respectively [32]:

$$n(\omega) = \sqrt{\left[\varepsilon_1(\omega) + |\varepsilon(\omega)|\right]/2},$$
 (13)

$$k(\omega) = \sqrt{[|\varepsilon(\omega)| - \varepsilon_1(\omega)]/2}.$$
 (14)

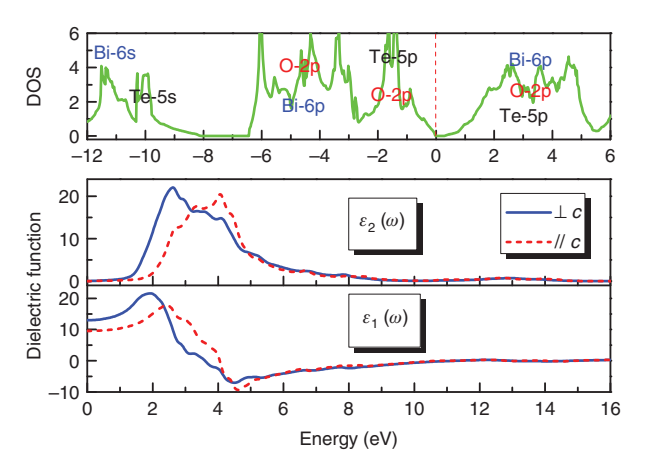


Figure 5: Dielectric curves in the directions perpendicular and parallel to the c axis of Bi₂O₂Te, together with the total DOS.

The calculated refraction and extinction curves of Bi₂O₂Te are given in Figure 6. Because the extinction function mainly reflects the absorption of light by medium when light propagates in it, its profile is very similar to that of $\varepsilon_2(\omega)$, which can also be explained by the electron transition as done previously. There are two broad peaks in the extinction curves: one is located at the energy range from 1.0 to 11.5 eV, which should be mainly caused by the electron transiting from the orbitals located between -6.0 and 0 eV to the permitted orbitals above the Fermi level. The second is at the energy range of 11.5-15.0 eV, which may be induced by the electrons transiting from the s orbitals at the energy range from -12 to -9 eV to the allowable orbitals above the Fermi level. From the calculated dielectric constants at zero frequency, one can obtain that $n_0 = n_{\perp} = 3.60$ and $n_e = n_{//} = 3.09$. Thus, Bi₂O₂Te has a birefringence of $\Delta n = n_e - n_o = -0.51 < 0$, which means that it is a negative uniaxial crystal. Its large birefringence can compare to those of some liquid crystals [33], implying that it can be used as tuning material in optical fields like those liquid crystals.

The absorption function denotes the losing energy of light when it transmits through a material by one unit thickness, which has a direct connection with the Joule heat produced in that material [34]. The reflection function weights the percentage of energy of light reflected from the surface of a material. The energy loss function measures the energy loss of a fast electron when it traverses in a homogeneous dielectric material [35]. The functions of absorption $\alpha(\omega)$, reflection $R(\omega)$ and energy loss $L(\omega)$ can be derived from the following expressions, respectively [32]:

$$\alpha(\omega) = 2\omega k(\omega)/c,\tag{15}$$

$$R(\omega) = \frac{[n(\omega) - 1]^2 + k(\omega)^2}{[n(\omega) + 1]^2 + k(\omega)^2},$$
 (16)

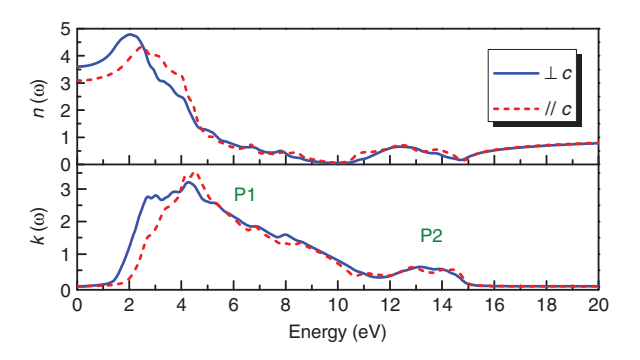


Figure 6: Refraction curves $n(\omega)$ and extinction curves $k(\omega)$ in the directions perpendicular and parallel to the c axis of Bi₂O₂Te.

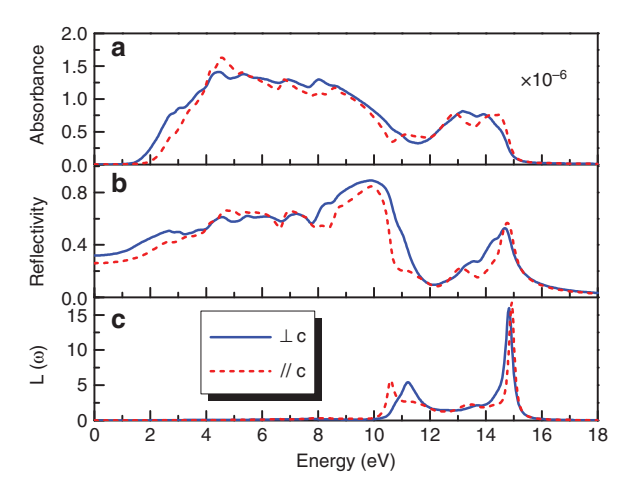


Figure 7: (a) Absorption (b) reflection and (c) energy loss $L(\omega)$ curves in the directions perpendicular and parallel to the c axis of Bi_2O_2Te .

$$L(\omega) = \frac{\varepsilon_2(\omega)^2}{\varepsilon_1(\omega)^2 + \varepsilon_2(\omega)^2},$$
 (17)

where *c* is the speed of light.

The computed absorption, reflection and energy loss curves of Bi₂O₂Te are illustrated in Figure 7. Because the absorption function is proportional to the extinction function, their figures seem alike. Bi₂O₂Te has non-zero absorbance >1.0 eV, which covers the energy scope of the visual light, meaning that Bi₂O₂Te is not transparent in this range. Reflection curves reveal that it has non-zero reflectivity in the energy range studied. In the intermediate energy range, classically 1-50 eV, the energy loss is mainly induced by single electron excitation and collective excitation [36]. Peaks in the energy loss curves reflect the plasma oscillation and the corresponding frequencies are called plasma frequencies, which can be obtained by letting $\varepsilon_1(\omega) = 0$ while restricting $\varepsilon_2(\omega) < 1$. A material is dielectric [$\varepsilon_1(\omega) > 0$] just above these frequencies, whereas it behaves like a metal $[\varepsilon_1(\omega) < 0]$ just below them [34]. There are two sharp peaks located at about 11 and 15 eV in the energy loss curves of Bi₂O₂Te, which correspond to plasma frequencies of about 2.6×10^{15} and 3.6×10^{15} Hz, respectively. The origins of these peaks in energy loss curves cannot be explained by the DOS because they are induced by the collective excitation of the electrons within the crystal.

4 Conclusions

The electronic, elastic and optical properties of ${\rm Bi_2O_2Te}$ were studied using the first-principles method. The results showed that ${\rm Bi_2O_2Te}$ is an indirect narrow band gap

semiconductor. The calculated DOS revealed that the top of the valence band is composed of Te 5p orbital, while the bottom of the conduction band is composed of Bi 6p orbital. Because of the orbital hybridisation and electron transfer between Bi and O, the Bi–O bonds have both ionic and covalent properties, providing forces to form the Bi–O layers. Electron transfer leads to the formation of the Te–Bi bonds, which glue the Bi–O layers forming the crystal.

The calculated elastic properties signify that Bi₂O₂Te is mechanically stable but anisotropic. The calculated bulk modulus is considerably larger than the shear modulus, indicating that the main factor limiting the mechanical stability of Bi_2O_2Te is the shear modulus. C_{44} and C_{13} are smallest among all the elastic constants, meaning that the crystal is easy to fracture along the c axis when subjected to a shear stress. Its Debye temperature is predicted to be 232.2 K and its melting point is estimated to be 1284.0 K. Its optical properties, such as the dielectric, refraction and absorption functions, were studied and the results indicated that Bi2O2Te is a negative uniaxial crystal with a birefringence of 0.51, which is desirable for tuning the frequency of light in optical fields. The origins and characteristics of the optical properties were also investigated.

Acknowledgements: This work was supported by the Student Research Training Program of the School of Physics and Engineering of Henan University of Science and Technology (grant no. 201803).

References

- [1] S. Murakami, Phys. Rev. Lett. 97, 236805 (2006).
- [2] L. E. Díaz-Sánchez, A. H. Romero, M. Cardona, R. K. Kremer, and X. Gonze, Phys. Rev. Lett. 99, 165504 (2007).
- [3] Y. S. Hor, A. Richardella, P. Roushan, Y. Xia, J. G. Checkelsky, et al., Phys. Rev. B 79, 195208 (2009).
- [4] H. Shi, D. Parker, M. H. Du, and D. Singh, J. Phys. Rev. Appl. 3, 014004 (2015).
- [5] Y. L. Chen, J. G. Analytis, J. H. Chu, Z. K. Liu, S. K. Mo, et al., Science 325, 178 (2009).
- [6] M. Z. Hasan and C. L. Kane, Rev. Mod. Phys. 82, 3045 (2010).
- [7] H. Boller, Monats. Chem. **104**, 916 (1973).
- [8] P. Ruleova, C. Drasar, P. Lostak, C. P. Li, S. Ballikaya, et al., Mater. Chem. Phys. 119, 299 (2010).
- [9] D. Guo, C. Hu, Y. Xi, and K. Zhang, J. Phys. Chem. C 117, 21597 (2013).
- [10] K. Zhang, C. Hu, X. Kang, S. Wang, Y. Xi, et al., Mater. Res. Bull. 48, 3968 (2013).
- [11] J. Wu, H. Yuan, M. Meng, C. Chen, Y. Sun, et al., Nat. Nanotech. 12, 530 (2017).
- [12] J. Yu and Q. Sun, Appl. Phys. Lett. 112, 053901 (2017).

- [13] A. L. J. Pereira, D. Santamaría-Perez, J. Ruiz-Fuertes, F. J. Manjon, V. P. Cuenca-Gotor, et al., J. Phys. Chem. C 122, 8853 (2018).
- [14] S. D. N. Luu and P. Vaqueiro, J. Solid State Chem. 226, 219 (2015).
- [15] M. Wu and X.C. Zeng, Nano Lett. 17, 6309 (2017).
- [16] C. Wang, G. Ding, X. Wu, S. Wei, and G. Gao, New J. Phys. 20, 123014 (2018).
- [17] G. Kresse and J. Furthmüller, Phys. Rev. B 54, 11169 (1996).
- [18] G. Kresse and D. Joubert, Phys. Rev. B 59, 1758 (1999).
- [19] J. P. Perdew, K. Burke, and M. Ernzerhof, Phys. Rev. Lett. 77, 3865 (1996).
- [20] H. J. Monkhorst and J. D. Pack, Phys. Rev. B 13, 5188 (1979).
- [21] F. Tran and P. Blaha, Phys. Rev. Lett. 102, 226401 (2009).
- [22] Z. L. Lv, H. L. Cui, H. Wang, X. H. Li, and G. F. Ji, Philos. Mag. 97, 743 (2017).
- [23] X. Hao, Y. Xu, Z. Wu, D. Zhou, X. Liu, et al., Phys. Rev. B 74, 224112 (2006).
- [24] W. Tang, E. Sanville, and G. Henkelman, J. Phys. Condens. Matter 21, 084204 (2009).

- [25] S. F. Pugh, Philos. Mag. 45, 833 (1954).
- [26] J. Haines, J. M. Leger, and G. Bocquillon, Annu. Rev. Mater. Res. 31, 1 (2001).
- [27] X. Q. Chen, H. Niu, D. Li, and Y. Li, Intermetallics 19, 1275 (2011).
- [28] I. Johnston, G. Keeler, R. Rollins, and S. Spicklemire, Solids State Physics Simulations, Wiley, New York 1996.
- [29] C. Detavernier, A. S. Özcan, J. Jordan-Sweet, E. A. Stach, J. Tersoff, et al., Nature 426, 641 (2003).
- [30] J. F. Nye, Physical Properties of Crystals, Clarendon Press, Oxford 1985.
- [31] M. Gajdoš, K. Hummer, G. Kresse, J. Furthmüller, and F. Bechstedt, Phys. Rev. B 73, 045112 (2006).
- [32] P. Nath, S. Chowdhury, D. Sanyal, and D. Jana, Carbon 73, 275
- [33] L. Wang, X. Lin, X. Liang, J. Wu, W. Hu, et al., Opt. Mater. Express 2, 1314 (2012).
- [34] X. Luo and B. Wang, J. Appl. Phys. 104, 053503 (2008).
- [35] D. Li, F. Ling, Z. Zhu, and X. Zhang, Physica B 406, 3299 (2011).
- [36] A. H. Reshak, Z. Charifi, and H. Baaziz, J. Solid State Chem. 183, 1290 (2010).